García, J., Molina, J.M., Trincado, J. (2020). Real Evaluation for Designing Sensor Fusion in UAV Platforms. *Information Fusion*, 63, pp. 136-152.

DOI: https://doi.org/10.1016/j.inffus.2020.06.003

Real Evaluation for Designing Sensor Fusion in UAV Platforms

Jesús García, Jose Manuel Molina, Jorge Trincado

jgherrer@inf.uc3m.es, molina@ia.uc3m.es, jtrincad@di.uc3m.es
Grupo de Inteligencia Artificial Aplicada of the University Carlos III de Madrid

Abstract: Evaluation of UAV systems is mostly based on simulation tools that are manually configured to define the trajectory (ground truth trajectory) for comparing with the system output. In this work, the authors present an original method to evaluate the performance of UAV platform in real situations without considering simulations. The proposed evaluation methodology allows calculating the system accuracy and robustness with a considerable number of samples, accumulating the performance of different missions in the same conditions. The main innovation is an alternative evaluation for designing sensor fusion parameters using real performance indicators of navigation accuracy in UAVs based on a commercially available flight controller and peripherals. This methodology and selected performance indicators allow to select the best parameters for the fusion system of a determined configuration of sensors and a predefined real mission not requiring ground truth. The selected platform is described highlighting the available sensors and data processing software, and the experimental methodology is proposed to characterize the sensor data fusion output. The results show in detail the presented performance metrics for a set of trajectories in order to determine the best choice of parameters using quality measurements of navigation output.

Keywords: UAVs sensor fusion; EKF; Real Data Analysis; System Design

1. Introduction

Unmanned Aerial Vehicles (UAVs) are controlled by a computer that integrates data from some electro-mechanical sensors and any local or global positioning system and applies control systems to change its position, orientation and velocity using the available locomotion system. The controller usually is an embedded microcontroller with appropriate interfaces to all vehicle components. As an example, PixHawk Px4 system integrates navigation data and software modules including fusion algorithms [1].

The main problem in navigation focuses on improving GNSS (Global Navigation Satellyte Systems) with the ability to provide accurate navigation output when this source of data becomes unavailable due to unexpected outages or problems derived from intentional attacks in GNSS denied environments such as signal interference (jamming) or fake signal generation (spoofing). Therefore, an approach based on the fusion of complementary sensors is essential, resorting to the fundamental equations of navigation and the characterization of the errors committed by each data source. This area has become popular due to the ubiquity of GNSS systems such as GPS (Global Positioning System) and the availability of inertial sensors based on inexpensive micro electro-mecanical systems (MEMS) components [2],[3],[4]. The integration of these complementary technologies allows compact and robust navigation solutions to determine attitude and location, so that the vehicle can determine its state in a robust way and use appropriate control techniques for autonomy. Other alternatives for non-dependence on the GNSS signal involve the deployment of autonomous localization systems such as the recognition of the environment by artificial vision [5] or location by means of several complementary sources [6], with the associated cost of developing a complementary infrastructure.

Complementary to navigation technologies, the use of lasers in combination with other range detection sensors (sonar, radar, video), allows to extend the navigation conditions and obstacle avoidance. In the air vehicles (UAVs), the integration requirements (consume, weight, dimensions) are much more restrictive but, even so, it is a line in continuous development [7],[8],[9]. Regarding protection against spoofing, there is also a noticeable research activity [10]. Protections include diverse strategies ranging from simple actions such as monitor the communication channel, to cryptographic authentication, discrimination based on the level of signal, time of arrival, multi-antenna systems, wave polarization, Doppler shift and arrival angle, etc., as described in [11], [12].

Therefore, research of robust and general techniques to integrate complementary data sources has become essential for this type of systems in order to provide reliable applications. The purpose of this research is the analysis of available equipment and experimental environments to validate the robustness of the theoretical solutions working in real conditions, and the contribution is based on a methodology and performance metrics to assess the performance in real-world conditions. The improvements in multi-sensor navigation must be based on the definition of parameters of the tracking system that should be adjusted to improve the output in a predefined set of missions with a set of available sensors. The methodology proposed in this paper assumes that real system adjustments will be based on a real platform with predefined flight missions so that, in this context, the best parameters could be obtained analyzing the real operation of sensors and real output. Simulation of UAV environments are not enough to evaluate in a thorough way these systems in real conditions of real missions. Accordingly to [13], evaluation tasks should be aligned with the user needs and how the fusion system meets the specifications. In this case of autonomous navigation, the accuracy and stability of fusion output, assessed by means of filter innovation and consistence, are priorized as target metrics to increase the relability of this critical function. The selection of parameters and quality metrics is a complex task, particularly in real applications, since there are not ground truth or a standard methodology for making the data fusion evaluation. There are numerous examples of output analysis of algorithms and configurations based on simulation, such as characterizing navigation errors [14], sensor fault detection [15], sensor integration in vehicular navigation [16] or simultaneous navigation and calibration [17]. Other works in UAV and vehicular navigation use experimental real data sets, usually illustrating the output in certain trajectories, in order to assess specific aspects such as robustness against GPS outages [18][19], estimation of magnitudes sensed from on-board sensors [20], impact of outliers in different solutions [21].

In this paper, the novelty of proposal is focused on the evaluation based on real data to avoid simulated evaluation and allow quantitave analysis of performance in real-world conditions in a systematic procedure. The main innovation is to test system parameters under real conditions in order to get comparative results. Before testing parameters, we define the UAV platform (type, sensors, tracking algorithms and control system). In this methodology the only parameters to be adjusted are related with estimation algorithms (and data fusion system) to improve the perception of the UAV. UAV type, sensors and control system keep constant in the proposed methodology. The steps of proposed methodology are: mission definition, mission execution, sensor data storage for each flight and, using this stored data, adjustment of data fusion algorithms to obtain the best filter parameters. Real data is used to optimize parameters of tracking filter, keeping constant type, sensors and control system. The briefing of this methodology for adapting filter parameters to real conditions is presented together with a systematic analysis of available real data. Section II presents a review of metrics for sensor fusion evaluation before introducing the proposed methodology and evaluation metrics. Section 3 presents the design problem for UAV navigation, highlighting the parameters of Extended Kalman Filter with impact in the performance. Section 4 introduces the selected

working platform, detailing the architecture of its software and the vehicles we have made to test its capacities and collect data. Section V explains the experimental environment, analyses the recorded sensor data and characterizes the PixHawk Px4 system filter and fusion algorithms following the presented methodology. Finally, section VI summarizes the conclusions derived from this work.

2. Evaluation of UAV Sensor Fusion in Real Conditions

In many real problems, simulated environments are used to define UAV sensors and the system parameters to optimize the system performance [14],[15],[16],[22],[23]. Some problems appear with this kind of methodologies, basically how to represent in simulation all effects appearing in real conditions and the way to evaluate the parameters configuration. UAV simulation have been applied to design the control subsystem for predefined missions, but simulation of real sensors is a major problem in this kind of approach. Real UAV conditions are not easy to model in simulators. UAVs are affected for atmospheric conditions and random movements due to control noise, so accurate simulation of input data is extremely complicated for designing system parameters.

2.1 Previous works

The validation and quality assessment of fusion system is a fundamental step in the development. Several authors establish quality metrics according the applications domain and their knowledge about the problem. A gap exists among the performance measures used in testing environments and the ones used in practical environments. Some authors have been carried some studies for comparing different metrics with ground truth and/or without ground truth [24][25][26][27][28], however these studies can be considered insufficient because the research community has shown a moderate application of them.

So, it is required to verify if the assessment suggestions on testing environments are also useful in practical environments. Besides, it is important to verify the use of "objective" measures, being independent from the application domain and from the human subjectivity. Avoid subjectivity is a complex task because user should be inside the test: some requirements must be fulfilled to select relevant information which is very dependent from the user and the domain application. Consequently, metrics show some dependence and a definition of the performance indicators that could be unified for various possible situations becomes very complex.

The quality dimensions can be grouped as quality metrics with ground truth and quality metrics without group truth:

A. Quality metrics with Ground Truth

A high number of metrics with ground truth have been applied in different fields such as multi-target tracking. However, the problem of this metrics is the application in real scenarios. Table 1 shows a set of metrics calculated using the ground truth, which are reported in the literature.

Table 1. Metrics based on ground truth

Metric	References
Accuracy: Root mean squared error, Average Euclidean error, Average Harmonic error, Average Geometric error / Completeness	[26]
# targets, #images, probability of (error, hit, FA, detection), confidence, attention, workload, delay variation, throughput, accuracy, positional accuracy.	[29]
RMSE of the position, MED of the position, AEE (Average Euclidean Error) of velocity	[28]
Kinematics Accuracy Detection performance = false track probability + probability of Missed Truth	[30]
Accuracy, completeness, opportunity, consistency	[31]
Accuracy, confidence, throughput, cost, opportunity, completeness, relevance, usability.	[32]
track error- range, track error – azimuth, track error –speed, track error heading. false track rate, false track length (updates) No. misclassified tracks, misclassified length (updates).	[33]
Accuracy: Root mean squared error of reconstructed position (transversal/longitudinal) and velocity (heading/groundspeed). Association: Percentage of unassociated plots in reconstructed trajectories, number of short trajectories	[34]

B. Quality metrics without Ground Truth

The quality metrics without ground truth are not widely reported, however after a systematic review, most of these classes of quality metrics have been applied in multi-target tracking applications. Table 3 and Table 4 show the global and local quality metrics respectively.

Table 3. Global Metrics without ground truth

Metric	References
Fusion break rate, Rate of fusion tracks, Track recombination rate	[35]

Delay, reaction time, timeliness, acquisition/run time, Update rate, cost, collection platforms, #assets	[29]

Table 4. Local Metrics without ground truth

Metric	References
Rate of non-associated data, Rate of premature removed tracks, Average residual	[35]
Delay, delay variation, Update Rate, cost	[29]
# Associated tracks	[33]
Association performance = track purity + track switches	[30]
Number of missed targets, track life time, Rate of False alarm number of false track per time window, Rate of track fragmentation, Track latency: confirmed track latency+tentaty track latency + dead track latency, Track redundancy, Number of spurious tracks, Number of false tracks, Total execution time.	[26]
Average number of broken tracks, Track continuity, Spurious track mean rate, Number of valid tracks	[26]
Consistency of estimators (visualization of histograms), stability of segmentation (visualization of mode of flight)	[36]

Therefore, as indicated in [35], the development of objective evaluation metrics with no available ground truth is a challenge yet for data fusion researchers. There are no well-established procedures to systematically evaluate sensor fusion systems beyond simulated conditions, making in many times difficult to predict performance in real-world conditions. After the revision of previous works, there are scarce global metrics without ground truth of fusion system, such as [34] where the metrics are fusion break rate, rate of fusion tracks and track recombination rate. This terminology considers "global" metrics as those assessing the global fusion system output, while "local" metrics evaluate specific outputs from individual sensor data processes in a decentralized fusion architecture. Some local metrics without ground truth are: rate of non-associated data, rate of premature deleted tracks and average residual [34], association performance metrics for track purity and track switches [33], or number of missed targets, track life time, rate of false alarms, rate of track fragmentation and track latency [26]. In particular, references [34],[36] refer to reconstruction algorithms used to evaluate

tracking systems. The quality of reconstruction is assessed mainly with simulated trajectories, and also visually inscpected with real datasets.

2.2 *Proposed Methodology*

In this scenario, the proposed methodology avoids simulated evaluation and tests directly the system parameters under real conditions. The first step of this methodology is the definition of the UAV platform, the type, cinematic characteristics, set of sensors, tracking algorithms and the control unit. Once the UAV platform is defined, the methodology is composed by the following steps, as displayed in Fig. 1:

1) **Design**: Mission definition. A specific mission is defined by means of a predefined trajectory containing a set of waypoints. A waypoint is a predetermined geographical position specified with global coordinates (latitude, longitude, altitude) and, following the navigation terminology, is used to predefine a change in direction, speed, or altitude along a certain trajectory, so it usually has associated a velocity vector (groundspeed and heading) or hold time if the speed is predifined to be zero. The flight controller takes waypoints as references to control the vehicle and follow the desired path. Basically, the procedures make use of both fly-over and fly-by waypoints. A fly-over waypoint is a waypoint that must be crossed vertically by an aircraft. A fly-by waypoint is defined as the intersection of two straight lines so the vehicle is expected to perform a transition from one path to another using a turn that "flies by" the waypoint but does not cross it. Specific parameters of fusion system are selected from a set of possible values. These specific parameters will be evaluated in real conditions by means of several flights. Waypoints are used to repeat the same flight several times to evaluate statistically the impact of some specific parameters.

2) **Execute**: Each time a flight of the UAV, passing through the predefined waypoints (mission), is carried out, the values of the sensor data are stored (position and velocity taken from GPS, inertial data, magnetometers, etc.), together with the system output (sensor fusion output, control errors, specific data processing results, etc.).

3) **Save**: A set of flights, with the same waypoints defining the mission, are carried out and the global data is stored in a log file. Data stored is the corresponding values of sensors data together with system output for specific parameters. Each log file is corresponding with specific parameters for filtering. At the end of the process, methodology generates a set of log files, one for each set of parameters. These log files are postprocessed offline.

4) **Analyze**: The best configuration of parameters is selected, analyzing the performance metrics for the set of flights carried out over the same waypoints (mission). The metrics defined in the following subsection are computed, a crucial point because evaluation needs to evaluate the sensor fusion performance based on real data not in ground truth.

5) **Apply**: The selected parameters are introduced in UAV system to perform real missions or refine the next tests to continue the design.

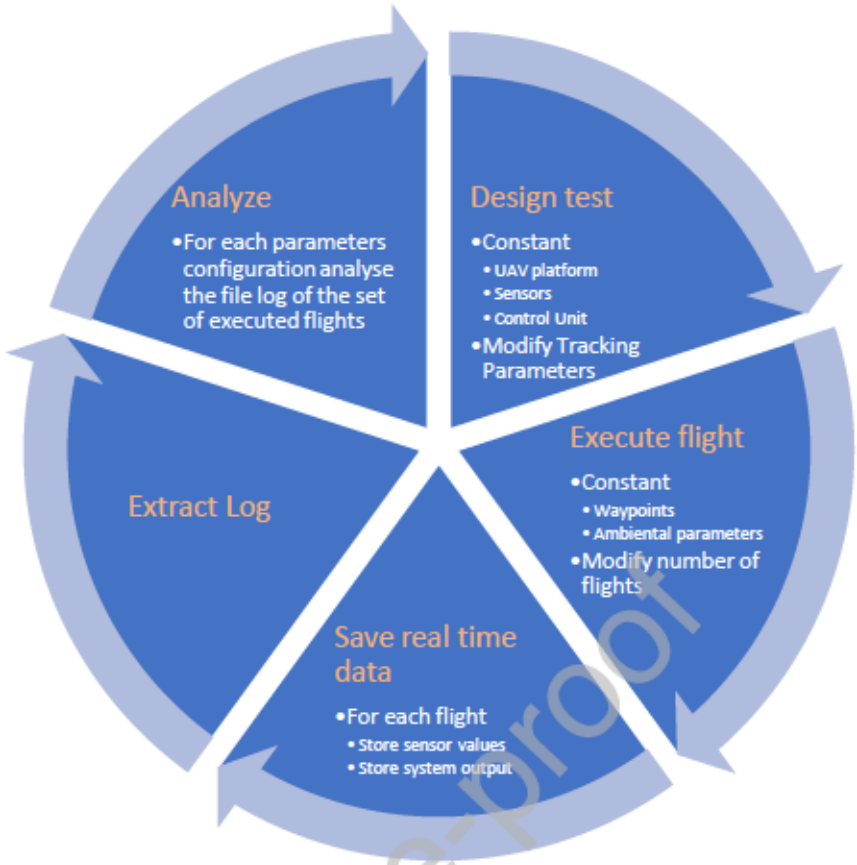

Figure 1: Real Evaluation Steps and Functionalities

The decision about "the best" parameters should be based in a set of indicators to evaluate the quality of the main components of the data fusion system. In this problem, since the plot association is not a problem, all sensor data are integrated in a single track, the sensor fusion performance is evaluated with the two global indicators: averaged innovations and fusion break rate. These metrics, detiled in next subsection, allow the validation of the designed system and decision of appropriate configuration parameters in complex scenarios.

2.2.1Averaged innovations

The innovation, or residual, is computed in the tracking filter each time an update is done for the prediction. For instance, for horizontal XY position, denoting with sub-index p the predicted state vector $(\hat{x}_p[k], \hat{y}_p[k]])$, and sub-index m for measurement $(x_m[k], y_m[k])$, both aligned at time k, and considering the average along a time window with N_T measurements, it is defined as:

$$r = \frac{1}{N_T} \sum_k (\hat{x}_p[k] - x_m[k])^2 + (\hat{y}_p[k] - y_m[k])^2 \quad (1)$$

The normalized innovation also employs the covariance matrices considering both the predicted and observation uncertainties, matrix S (known as Mahalanobis distance). The averaged value of normalized innovations defined as:

$$r_n = \frac{1}{N_T} \sum_k [\hat{x}_p[k] - x_m[k] \quad \hat{y}_p[k] - y_m[k]] \, S \; [k]^{-1} \begin{bmatrix} \hat{x}_p[k] - x_m[k] \\ \hat{y}_p[k] - y_m[k] \end{bmatrix} \tag{2}$$

Being S the sum of covariances in position for predicted vector and measurements (assuming their errors are independent):

$$S = P_p[k] + R[k] = \begin{bmatrix} \sigma^2_{x_p}[k] & \sigma_{x_p y_p}[k] \\ \sigma_{x_p y_p}[k] & \sigma^2_{y_p}[k] \end{bmatrix} + \begin{bmatrix} \sigma^2_{x_m}[k] & \sigma_{x_m y_m}[k] \\ \sigma_{x_m y_m}[k] & \sigma^2_{y_m}[k] \end{bmatrix} \tag{3}$$

This value is a-dimensional, and represents the discrepancy between observations and predictions, averaged along the measurements contained in N_T. It is interesting to notice that covariance matrix for observation noise, R, is dependent on the sensor (in this case, mainly GPS), but the predicted covariance, Pp, depends on the assumed uncertainty for the model, as will be detailed in section 3. This implies that a very high value for Pp would produce very low values of residual r_n, giving an incorrect indication of the quality metric.

This problem can be addressed validating the consistency of residual r_n. The normaized residual follows a normalized Chi-squared distribution with parameter DF (degrees of freedom) given by twice the number of 2D measurements averaged minus the dimension of *S* (4). So, for a valid model, r_n should behave with this distribution:

$$r_n \sim \frac{1}{N_T} \chi^2_{(2N_T - 4)} \tag{4}$$

So, the value should not be too far from theoretical mean $\mu = 2 - \frac{4}{N_T}$ in order to validate the consistency of predicted covariance, taking the lower and higher bounds of confidence interval from the χ^2 distribution, as shown in [37] for a similar problem.

Sometimes, if full covariance matrices are not available, a simplification is done and only the variances (diagonal terms) are considered:

$$r_n = \frac{1}{N_T} \sum_k \left(\frac{(\hat{x}_p[k] - x_m[k])^2}{\sigma^2_{xp} + \sigma^2_{xm}} + \frac{(\hat{y}_p[k] - y_m[k])^2}{\sigma^2_{yp} + \sigma^2_{ym}} \right) \tag{5}$$

This residual in horizontal plane has been defined using usual XY coordinates in plane, usually provided by the tracking filter. Sometimes, a more specific separation of components in transversal and longitudinal components of vehicle could be computed (as in [34]), providing errors more informative about specific aspects of missions, for instance the effect of control loop in some maneuvers. This work is focused on asessing the estimation errors, leaving the analysis of control error for possible extensions in future works.

With respect to vertical residual, it is computed in the same way as a 1D magnitude using the vertical deviations of prediction with respect to observations:

$$r_{nh} = \frac{1}{N_T} \sum_k \frac{(\hat{z}_p[k] - z_m[k])^2}{\sigma_{zp}^2 + \sigma_{zm}^2} \quad (6)$$

(the same comments about model validation for parameters $\sigma_{xp}^2, \sigma_{yp}^2, \sigma_{zp}^2, \sigma_{xm}^2, \sigma_{ym}^2, \sigma_{zm}^2$ can be applied to the values in previous equations).

2.2.2 Fusion break rate

The rate of fusion break, t_{FB}, is the number of times some navigation observation is declared as inconsistent in the integrity analysis and therefore de-fused (the less consistent component is removed from the system track). This may lead to tracker re-initialization or keep the system track with a component less, the faulty sensor. It is computed as:

$$t_{FB} = \frac{\sum_i \{\#(o_i) | o_i \text{ is inconsistent observation}\}}{N_T} \quad (7)$$

Being o_i each observation declared as inconsistent within the interval of of N_T measurements. It is obtained counting the total number of fusion break events during the interval. The test to decide the removal of a data source is done using again the normalized innovation, with a typical threshold value of 5 times the standard deviation.

3. Design parameters for UAV navigation filter: centralized EKF algorithm

The sensor fusion system is based on a loosely coupled architecture, which uses GPS position and velocity measurements to aid the INS, typically used in most of navigation solutions based on sensor fusion [15],[18],[36],[22],[38]. In this way, the IMU sensors are used extrapolate position, velocity, and attitude at high frequency (50 Hz), while updates from GPS measurements at lower frequency (1 Hz) allows refinement of cinematic estimates and inertial sensor biases. Other proposals for multisensor navigation besides EKF are unscented Kalman (UKF) and Interacting Multiple Model (IMM) filters. The UKF non-linear character is employed to include some state constraints, such as surface geometry in road navigation [40]. In [41] a Interacting Multiple Model (IMM) is used. The state vector is updated with different dynamic models and IMM combination: constant velocity (CV), constant acceleration (CA), and constant turn (CT) models, a similar structure as used in sensor fusion with sets of models known a priori . The identification of stops situations is very useful and can be applied to activate calibration processes, for instance knowing that during stops, accelerations and rotation rates should be zero [40]. Besides, the problem of designing complex sensor fusion systems has been addressed from the point of view of machine learning. An approach to contextual aspects of GNSS/INS sources is presented in [40], or [41] presents the use of dynamic Neural Networks to build models of INS errors before combination with GPS data to facilitate adaptation with time-varying errors

In any case, independently of the selected sensor fusion algorithm, the estimated state vector resulting in the output for the GNSS/INS filter usually contains the attitude vector (represented alternatively with a quaternion or Euler angles vector), 3D position and velocity and the bias terms for gyro accelerometer measurements.

In this work, we have selected a representative dynamic model integrating local sensed inputs (accelarion and turns), absolute positions (GNSS data) and the dynamics of sensor biases, with appropriatey uncertainty models for the predictions. Most of solutions in literature share this global approach, with multiple variations in the particular coordinates and equations dynamics, although the meaning of parameters is basically the same. The selected coordinate frame for position and velocity in this solution is the ENU frame (East, North, Down) with respect to the tangent plan with origin defined by the arming point in the start of the mission. Other alternatives appear when independent modules with subsets of sensors are available to estimate attitude and cinematics with parallel filters [23], a robust solution but only available when the number of sensors is enough to group then in independent modules.

This state vector allows the continuous estimation of cinematics and attitude of vehicle together with the inertial sensor biases, represented in a 16D vector which contains 3D position and velocity, attitude (represented with 4D quaternion q_n) and 3D biases corrections for acceleration and angular rate in body frame, respectively b_a and b_w:

$$\mathbf{x}[k] = \left[\mathbf{p}_n{}^t[k] \quad \mathbf{v}_n{}^t[k] \quad \mathbf{q}_n{}^t[k] \quad \mathbf{b}_a{}^t[k] \quad \mathbf{b}_\omega{}^t[k]\right]^t \tag{8}$$

The orientation is usually computed with respect to the reference origin point taken at the mission arming point when engines are started (O in figure), with local ENU (East-North-Up) coordinates used to represent the vehicle position, velocity and orientation.

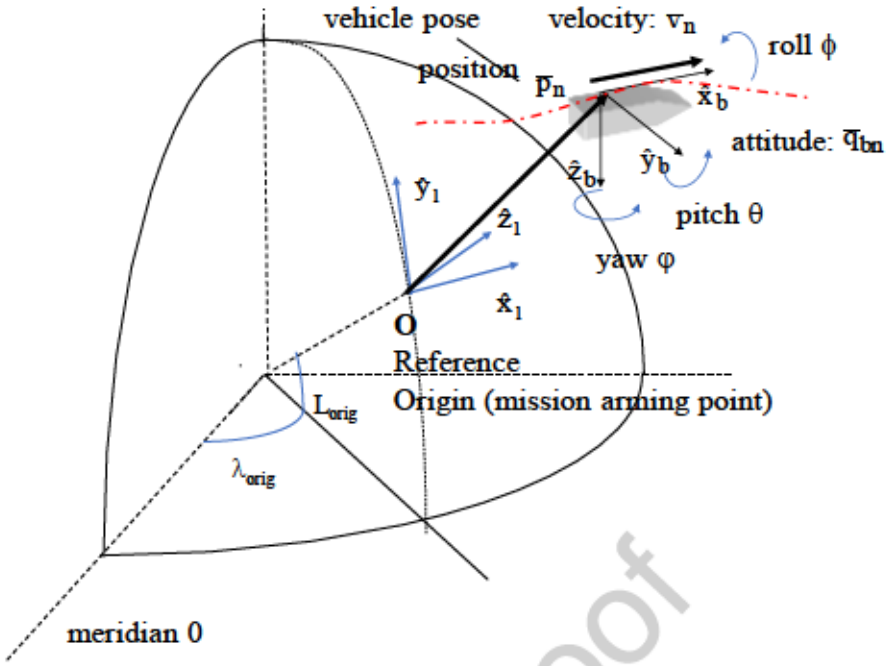

Figure 2: DCM inertial measurement conversion

As shown in Fig 3, the position and velocity are usually expressed in the inertial ENU frame (sub-index n) and the sensor biases expressed in the body-fixed frame. The state vector can be extended to include bias in barometric height, $\bar{x}^E[k] = \left[\bar{x}[k]^t \quad b_h[k]\right]^t$ if a barometer is available, to integrate also this source of measurements.

So, the EKF fusion algorithm processes all available measurements in a centralized module: GPS, barometric height sensors, and the input of IMU readings with local body-frame sensed acceleration and angular rates. As we have mentioned, GPS and barometer inputs (z_{GPS}, z_{baro}) are considered, within Kalman inference mechanism, as "observations", while IMU inputs (a_m, w_m) are considered as "control inputs":

$$z_{GPS}[k] = \begin{bmatrix} x_m[k] \\ y_m[k] \\ z_m[k] \end{bmatrix} = \begin{bmatrix} x[k] \\ y[k] \\ z[k] \end{bmatrix} + \begin{bmatrix} n_{GPSx}[k] \\ n_{GPSy}[k] \\ n_{GPSz}[k] \end{bmatrix} \tag{8}$$

$$z_{baro}[k] = [z_m[k]] = z[k] + b_H[k] + n_{BARz}[k] \tag{10}$$

Being n_{GPS} the obvservation noise of GPS 3D measurements, n_{BARz} the observation noise in the barometric height, and b_H the corresponding bias in this magnitude. The input control contains the ideal magnitudes of 3D accelerations and angular rates expressed in the body-fixed local frame, respectively $\bar{a}_u[k]$ and $\bar{\omega}_u[k]$:

$$u[k] = \left[\bar{a}_u{}^t[k] \quad \bar{\omega}_u{}^t[k]\right]^t \tag{11}$$

This input control is related to available IMU measurements at k-th time $(\bar{a}_m[k], \bar{\omega}_m[k])$, which must be corrected with the respective estimated biases in the state vector.

$$\begin{aligned}
&\hat{u}[k] = \left[\hat{a}_b{}^t[k] \quad \hat{\omega}_b{}^t[k]\right]^t \\
&\hat{a}_b[k] = \hat{a}_m[k] - \bar{b}_a[k] \\
&\hat{\omega}_b[k] \equiv \left[\hat{\omega}_p[k] \quad \hat{\omega}_q[k] \quad \hat{\omega}_r[k]\right]^t = \hat{\omega}_m[k] - C_b^n[k]\bar{\omega}_{En} - \bar{b}_\omega[k]
\end{aligned} \tag{12}$$

Besides, in the case of body angular rate, also the Coriollis effect, $\bar{\omega}_{En}$, is subtracted to generate the corrected input control, projected through the Body-to-ENU frames conversion matrix, $C_b^n[k]$. This projection matrix is direclty obtained from the vehicle attitude expressed in quaternion vector:

$$C_n^b[k] = \begin{bmatrix}
q_0[k]^2 + q_1[k]^2 - q_2[k]^2 - q_3[k]^2 & 2(q_1[k]q_2[k] - q_0[k]q_3[k]) & 2(q_1[k]q_3[k] + q_0[k]q_2[k]) \\
2(q_1[k]q_2[k] + q_0[k]q_3[k]) & q_0[k]^2 - q_1[k]^2 + q_2[k]^2 - q_3[k]^2 & 2(q_2[k]q_3[k] - q_0[k]q_1[k]) \\
2(q_1[k]q_3[k] - q_0[k]q_2[k]) & 2(q_2[k]q_3[k] + q_0[k]q_1[k]) & q_0[k]^2 - q_1[k]^2 - q_2[k]^2 + q_3[k]^2
\end{bmatrix} \tag{13}$$

The EKF requires a system model described by the state vector and a dynamic stochastic model to describe its evolution with time:

$$\dot{\bar{x}}(t) = \frac{\bar{x}(t)}{dt} = \bar{y}(t, \bar{x}(t), \bar{u}(t), \bar{v}(t)) \tag{14}$$

being $\bar{u}(t)$ the control input (deterministic) and $\bar{v}(t)$ is the plant noise process (unobservable noise). The first term $\bar{u}(t)$ is related to the observations provided by inertial sensors as indicated above, which include a certain noise error, while $\bar{v}(t)$ is an additional noise model to take into account deviations from the predictions. The prediction equations resulting from the model are obtained after integration of differential equation, a well-known model [42] is obtained for this problem with the following (non-linear) equations:

$$x_n[k+1] = f(x_n[k], u(t)) = F(x_n[k], u(t))\,x_n[k] + u(x_n[k]):$$

$$\begin{bmatrix} p_n[k+1] \\ v_n[k+1] \\ q_n[k+1] \\ \bar{b}_a[k+1] \\ \bar{b}_\omega[k+1] \end{bmatrix} = \begin{bmatrix} I_3 & \Delta t I_3 & 0_{3x4} & 0_{3x3} & 0_{3x3} \\ 0_{3x3} & I_3 & 0_{3x4} & 0_{3x3} & 0_{3x3} \\ 0_{4x3} & 0_{4x3} & A[k] & 0_{4x3} & 0_{3x3} \\ 0_{3x3} & 0_{3x3} & 0_{3x4} & I_3 & 0_{3x3} \\ 0_{3x3} & 0_{3x3} & 0_{3x4} & 0_{3x3} & I_3 \end{bmatrix} \begin{bmatrix} p_n[k] \\ v_n[k] \\ q_n[k] \\ \bar{b}_a[k] \\ \bar{b}_\omega[k] \end{bmatrix} + \Delta t \begin{bmatrix} 0_{3x1} \\ U[k] \\ 0_{4x1} \\ 0_{3x1} \\ 0_{3x1} \end{bmatrix} \tag{15}$$

where A[k] is the attitude transition matrix corresponding to the object attitude represented with quaternion, which depends on the components of corrected angular velocity in body frame, $\bar{\omega}_b[k] = \left[\omega_p[k] \quad \omega_q[k] \quad \omega_r[k]\right]$:

$$A[k] = \left(I_4 \cos(s[k]) - \frac{1}{2}\Delta t\,\Omega[k]\frac{\sin(s[k])}{s[k]} \right) \tag{16}$$

Being the terms in previous equation computed as:

$$\Omega[k]=\begin{bmatrix} 0 & \omega_p[k] & \omega_q[k] & \omega_r[k] \\ -\omega_p[k] & 0 & -\omega_r[k] & \omega_q[k] \\ -\omega_q[k] & \omega_r[k] & 0 & -\omega_{p[k]} \\ -\omega_r[k] & -\omega_q[k] & \omega_p[k] & 0 \end{bmatrix} \tag{17}$$

$$s[k]=\frac{1}{2}\Delta t\sqrt{(\omega_p[k])^2+(\omega_q[k])^2+(\omega_r[k])^2} \tag{18}$$

And, finally, U[k] is the correction in the velocity computed from the control input, corresponding to acceleration vector, expressed in inertial frame and projected to ENU frame, affected by the gravitational effect:

$$U[k]=C_n^b[k]\,\bar{a}_b[k]+\bar{g} \tag{19}$$

With this dynamic model, the Extended Kalman Filter approximates the predictions and their covariance matrix with a first-order approximation for the non-linear functions of prediction model, $\bar{f}(.)$, and projection to the measurement space, $\bar{h}(.)$:

$$\begin{aligned} \bar{x}_n[k\,|\,k-1] &= \bar{f}(\bar{x}_n[k],\ \bar{u}[k],\ \bar{v}[k]) \\ z_n[k] &= \bar{h}(\bar{x}_n[k],\ \bar{w}[k]) \end{aligned} \tag{20}$$

being w[k] the observation noise process, and v[k] the system process noise to characterize uncertainty in the predictions. The prediction equations of Extended Kalman Filter are used to propagate the state vector and covariance matrix:

$$\begin{aligned} \hat{x}[k\,|\,k-1] &= f(\hat{x}[k-1\,|\,k-1],\hat{u}[k-1]) \\ P[k\,|\,k-1] &= F[k]P[k-1|k-1]F^T[k]+V[k]Q_u[k-1]V^T[k-1]+Q_p[k-1] \end{aligned} \tag{21}$$

The matrices F, V, H are computed with the Jacobean operators applied to the model functions f and h:

$$F_{[i,j]}=\frac{\delta f_{[i]}}{\delta x_{[j]}}(x(t),q(t),u(t),t) \tag{22}$$

$$V_{[i,j]}=\frac{\delta f_{[i]}}{\delta u_{[j]}}(x(t),q(t),u(t),t) \tag{23}$$

$$H_{[i,j]}=\frac{\delta h_{[i]}}{\delta x_{[j]}}(x(t),w(t)) \tag{24}$$

The covariance matrix for process noise, Q, is separated in two terms: Q_p, corresponding to uncertainty in predictions and Q_u, projecting the errors of inertial sensors to the state vector.

$$Q[k]=V[k]Q_u[k-1]V^T[k-1]+Q_p[k-1]$$

$$Q[k] = V[k]\begin{bmatrix} 0_{10x10} & 0_{10x3} & 0_{10x3} \\ 0_{3x10} & q_{am}^2 I_3 & 0 \\ 0_{3x10} & 0 & q_{wm}^2 I_3 \end{bmatrix} V^T[k] + \begin{bmatrix} 0_{10x10} & 0_{10x3} & 0_{10x3} \\ 0_{3x10} & q_{ap}^2 I_3 & 0 \\ 0_{3x10} & 0 & q_{wp}^2 I_3 \end{bmatrix} \quad (25)$$

being $q_{am}^2, q_{wm}^2, q_{ap}^2, q_{wp}^2$ the model parameters used to tune the system response by adaptation of the plant-noise process Q[k]. The first two are used to model the uncertainty of IMU sensors, projected through V matrix to state vector, and the last two are direct models of prediction uncertainty for the assumed model of smooth variation of inertial sensor biases.

Some of this parameters were tuned in the available experimental system with the methodology presented, as will be indicated in the following section.

Finaly, given the prediction model detailed above, the "update" phase of extended Kalman filter is given by the classical EKF equations:

$$K[k] = P[k|k-1]H[k]^t\left(H[k]P[k|k-1]H[k]^T + R[k]\right)^{-1} \quad (26)$$

$$\hat{x}[k|k] = \hat{x}[k|k-1] + K[k](z[k] - h(x[k|k-1])) \quad (27)$$

$$P[k|k] = P[k|k-1](I - K[k]H[k]) \quad (28)$$

where the R[k] matrix in EKF update equations consider the noise in measurement observations:

$$R_{GPS} = \begin{bmatrix} \sigma_h^2 & 0 & 0 \\ 0 & \sigma_h^2 & 0 \\ 0 & 0 & \sigma_v^2 \end{bmatrix} \quad (29)$$

$$R_{BAR} = \sigma_{bar}^2 \quad (30)$$

Being σ_h^2, σ_v^2 the variance in horizontal and vertical errors of GPS positions, respectively, and σ_{bar}^2 the variance in barometric height.

Therefore, the EKF filter used for sensor fusion depends on two sets of parameters wich are sensor noise and plant noise. The terms in equation 21 correspond to the plant noise, used to stabilize the filter and avoid becoming too confident in its own predictions with respect to measurements. Both the estimation of cinematic parameters and sensor biases depend on chosing appropriate parameters characterizing noise in sensor data and uncertainty in prediction (process noise). Espeficiallly, process noise parameters affect to the predicted error covariance and have critical impact in the weights given to the sensor observations with respect to the predicted estimates. A higher value for these parameters implies higher values of predicted covariance and so higher gain to observations (since the confidence on prediction decreases). Conversely, lower values imply lower gain to observations (higher confidence on predictions). For instance, if GPS position noise parameters are set to very small values compared to INS prediction errors, it will produce frequent changes of position and attitude during vehicle hoover state. In the same way, low values for GPS velocity noise will cause the filter roll and pitch angles to be noisy, probably affecting to the vehicle motion up and down. In the next section, we will identify the available parameters of EKF in the selected platfor UAV experimentation.

4. The PixHawk and PX4 UAV System

Unmanned vehicles are used to execute predetermined missions such as data collection, event detection, surveillance tasks, etc., and for that they must be able to control their position and orientation (pose) by means of automatic control algorithms. They are controlled by a

computer that integrates data from available electro-mechanical sensors and external GNSS positioning system and applies output control systems to change its location using any locomotion system. This controller is usually an embedded microcontroller that performs the core of all vehicle components.

The experimentation and analysis have been done with the PixHawk flight controller. It is an open-hardware computer designed by 3D Robotics specifically to create autopilot vehicles, integrating PX4FMU and PX4IO boards in the same PCB (Printed Circuit Board). The integrated software with sensor data processing and flight control algorithms allows access to a rich set of parameters driving their performance. This is the main reason of using this solution to illustrate the proposed methodology and analyse the results obtained with different parameters.

4.1 Sensors and data sources

The PixHawk board has several sensors integrated to sense the local motion and environment of vehicle (accelerations, rates of turn, altitude, magnetic field, etc.), indicated in Table 3. They serve as data sources to the PX4 stack and also include some data processing functions, such as a digital motion processing (DMP) with programable low pass filters used MPU-6000 data.

Table 3 Sensors Integrated in the PixHawk Board

Sensor	Type	Axes	Scale	ADC accuracy	Data rate
L3GD20H	gyroscope	3	2000 dps	16 bits	760 Hz
LSM303D	accelerometer/ magnetometer	6	± 16g / ± 2gauss	16 bits	1600 Hz/ 100 Hz
MPU-6000	accelerometer/ gyroscope	6	± 16g / 2000 dps	16 bits	1000 Hz/ 8000 Hz
MS5611	barometer	1	1200 mbar	24 bits	1000 Hz

Besides the sensors integrated in the board, PixHawk counts with high connectivity for external devices and peripherals to increase the vehicle capabilities. At the right side, there are some specific connectors for certain peripherals, such as the two connectors for telemetry communication, one for GPS, and one Spektrum receiver socket. At the left side, there are some general-purpose ports and buses like two universal asynchronous receiver transmitter (UART) ports, two serial peripheral interfaces (SPI), one inter-integrated (I2C) connector, one universal serial bus (USB) connector, one controller area network (CAN) bus connector and 3.3V and 6.6V ADC connectors. The standard configuration of a PixHawk UAV counts with interfaces to external sensors specified in Table 4:

Table 4. Additional sensors wired to the PixHawk

Sensor	Type	Interface	Range	Accuracy	Data rate
Ublox Neo 6M	GPS	GPS port	x	2.5m	<3s
HMC5883	Magnetometer	I2C	± 16G	±12MG	1600 Hz

Flow Sensor	Optical	I2C	x	<0.5m	250Hz
shield	flow/gyroscope				
Range finder	Ultrasonic sonar	I2C	0-6m	0.5cm	1000 Hz
Lidar lite	Pointer lidar	I2C	0-40m	±2.5cm	1-500Hz

The complete set of sensors allow enhancing navigation capabilities and increase the accuracy of the stabilization system measurements, what is quite important when we want to create an unmanned vehicle, because it allows a more faithful image of the environment. Sensor inputs are processed by flight controller, together with commands received from telemetry, and this is used to control the motion through appropriate signals sent to the motors through electronic speed controllers (ESC).

4.2 Software for Flight Control and Data Processing

PX4 is the control software of PixHawk processor. It is a real-time operating system based on NuttX architecture and consists of two main layers: PX4 Flight Stack and PX4 Middleware. PX4 Flight Stack is the complete collection of applications embedded in PixHawk hardware for drone control, while PX4 Middleware is the interface that allows the flow of data from sensors to applications through a publish/subscribe system called uORB. uORB allows to publish the data coming from the sensors and make them available to the applications of the Flight Stack, obtaining a reactive system and totally parallelized.

Regarding data processing, Px4 integrates an AHRS (attitude and heading reference system) that implements different algorithms to estimate the vehicle attitude and creates a direction vector used as reference for vehicle displacement. Fig. 3 shows the process flow from sensors to actuators used in this research, to give a general view of the whole flight control system [39]. The outstanding module is the Flight Controller where the navigation input is provided by sensor fusion based on the extended Kalman filter (EKF). It estimates the vehicle position, velocity and angular orientation, which are compared with the intendend trajectory provided by the navigator based on the missions sent from ground station. The controller is based on proportional-integrative-derivative (PID) modules which are mixed with control inputs from radio control to generate the individual inputs sent to each electronic speed controller.

The focus of this work is in the performance of sensor fusion algorithms (highlighted in red in Fig. 3), with apropriate analysis based on real data and impact of the parameters used in this module in the accuracy of navigation system.

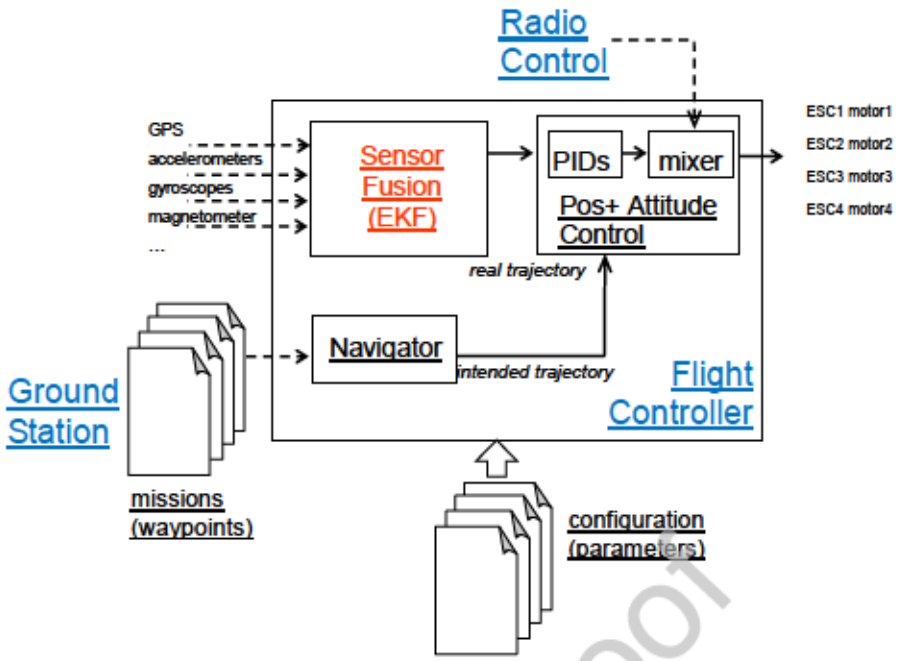

Figure 3: Main components in flight controller

The basic components that are used to compute the navigation solution (position, velocity and attitude) during the flights are indicated below:

4.2.1 Direction Cosine Matrix (DCM)

This program allows the analysis of the triaxial accelerometers and gyroscopes data to obtain a Direction Cosine Matrix [45]. It makes possible the conversion of real-time measurements referred to the vehicle body frame into instantaneous orientation parameters of the vehicle to deliver roll, pitch and yaw angles (see Fig. 3) or variations (as quaternion vector used in the fusion filter).

4.2.2 Inertial Navigation System (INS)

This algorithm computes the movement and corrections based on onboard sensors and allows the vehicle to extrapolate its position between points using the DCM input. It is used to estimate the vehicle attitude with high frequency, so it is especially useful to complement the global position obtained from the GPS data.

4.2.3 Extended Kalman Filter (EKF)

Finally, the EKF is the algorithm fusing all measurements, integrating the inputs from DCM and INS to carry out the predictions between GPS observations. It considers the noise affecting to all measurements in the estimation of attitude and cinematic parameters to increases the accuracy and consistence of the output, even when the vehicle losses the GPS signal in certain time intervals. The Px4 system counts with several Extended Kalman Filter algorithms to process all sensor data (EKF1, EKF2, EKF3) in a compensation function that depends of the specific noise, availability and accuracy characterization of each sensor, throwing high accuracy estimations of the vehicle attitude. It can apply different EKF solutions running in parallel, using different sensor measurements and states. Table 5 shows the three available EKF modes:

TABLE 5. Px4 Extended Kalman Filters

Name	Specification
EKF1	Only use the DCM for attitude control and the Inertial navigation for AHRS reckoning for position control
EKF2	Use the GPS for 3D velocity and position. The GPS altitude could be used if barometer data is very noisy.
EKF3	If there is no GPS, it can use optical flow to estimate 3D velocity and position.

Therefore, AHRS does not use a single Kalman Filter, but it is able to select the best EKF mode for each situation and execute both EKF1 and EKF2 in parallel if it is necessary.

As mentioned, all available sensors are fused to estimate the position, velocity, and angular orientation by means of EKF. This algorithm has parameters used in the models of sensor measurements and and prediction errors. Basically, when sensor noise parameters are high in comparison to predictions, the filter gives less weights to the measurements, with potential delays and deviations during maneuvers, while small noise parameters produce high weighting, and consequently the filter will overreact to noise in the measurements. Regarding control, a proportional–integral–derivative (PID) controller is used to controll the multi-rotor angular orientation, with independent controllers for roll, pitch, and yaw. Each controller calculates the demanded angle rate based on differences between measured and demanded values of each angle, affected also by certain time constant parameters of controllers which regulate the system stability and reaction to changes.

This work is focused on sensor fusion performance, and the analysis considers the impact of some of the key parameters of EKF used for estimation of navigation solution, described in section 3. The parameters controlling the EKF performance are indicated in Table 6.

TABLE 6. Px4 prediction noise parameters of EKF2

Name	Description	Default values
EKF2_ACC_B_NOISE	Process noise for IMU accel. bias prediction	0.003 m/s^3
EKF2_GYR_B_NOISE	Process noise for IMU rate gyro bias prediction	0.001 rad/s^2
EKF2_ACC_NOISE	Accelerometer noise for covariance prediction	0.35 m/s/s

EKF2_GYR_NOISE	Rate gyro noise for covariance prediction	0.015 rad/s

With respect to sensors noise parameters, they have been adjusted considering the accuracy specifications from sensor providers. The default values for sensor noise were used in all flights, as presented in Table 7

TABLE 7. SENSOR MEASUREMENT PARAMETERS OF EKF2

Name	Description	Values
EKF2_BARO_NOISE	barometric altitude	2.0m
EKF2_GPS_P_NOISE	gps position	0.5m
EKF2_GPS_V_NOISE	gps horizontal velocity	0.5 m/s
EKF2_MAG_NOISE	magnetometer 3-axis	5.0e-2 Gauss
LPE_ACC_XY	Accelerometer xy noise density	0.012 m/s^2/ sqrt(Hz)
LPE_ACC_Z	Accelerometer z noise density	0.02 m/s^2/ sqrt(Hz)
EKF2_HEAD_NOISE	noise for magnetic heading fusion	0.3 rad

Finally, the sensor fusion logic includes protection values for self-assessment of performance, as mentioned in section 2 (fusion break events). A data source will be de-fused each time the threshold value for residuals are exceeded, being the default value 5 times the standard deviation, as shown in Table 8.

Table 8. Fusion Gate Parameters of EKF

Name	Description	Values
EKF2_GPS_P_GATE	Gate size for GPS horizontal position fusion	5.0SD
EKF2_GPS_V_GATE	Gate size for GPS velocity fusion	5.0 SD
EKF2_BARO_GATE	Gate size for barometric and GPS height fusion	5.0 SD
EKF2_RNG_GATE	Gate size for range finder fusion	5.0 SD
EKF2_EV_GATE	Gate size for vision estimate fusion	5.0 SD

5. Experimental Environment and Sensor Data Analysis

5.1 Data acquisition

The process of data acquisition was based on several flight test missions that have taken place on circuits like the one sketched in Fig. 4.

Mission circuit design

Real mission execution

Figure 4: Test circuit diagram

All flights were carried out with auto-pilot mode and supervised by human controller to change the mode of flight if needed. For each specified mission, we applied different configuration parameters to analyze the performance differences between each setting up of tracking filters.

Besides these flights to assess the entire system (sensor fusion and flight control working together), previous tests were carried out to test specific sensors and configurations, as indicated in Table 9. The static test has been performed on the floor to avoid displacements and vibrations that could disturb the readings

TABLE 9. TEST PERFORMED OVER THE SAME CIRCUIT

Name	Specification
Static test without propellers	Accelerometers and gyroscopes, noise
Static test on idle	Accelerometers and gyroscopes, noise
Unmanned flight test	GPS, inertial navigation system
Unmanned hold test	GPS, Flow Sensor, DCM
Manual flight test	PID and configuration parameters

5.2 Data Characterization

Before exploiting sensor data for navigation enhancement, it is important to know the behaviour, limitations and main characteristics of the data we are working with, to establish a measure of the confidence and the consistence of the data. These properties are conditioned by the sensors and measurement processes. The logged data is very useful to debug the estimation algorithms and the flight performance. In this work we have focused in data used to explain the position estimations, the navigation system performance and the filter capabilities. Table 10 shows the data analysis for the main data sources available [46].

Table 10. Data characterization

Sensor	Source	Range	Accuracy	Data rate
Raw X,Y,Z accelerometer	L3GD20H MPU-6000	± 16g	± 0.02g	8000Hz
Raw X Y Z gyroscope	L3GD20H MPU-6000	[±2000] deg/s	± 3deg/s	8000Hz
Roll, Pitch, Yaw	DCM over Accel/Gyro	[0,180]º	± 0.05deg	1600Hz
Heading	DCM over magnetometer	[0,360]º	± 1.5deg	1000 Hz
Atm. Pressure	MS5611	[10,1200]Hpa	± 1.2Hpa	1000Hz
Sonar Floor		[0,6]m	± 0.02m	
Estimated local position terms	INS	Different		1000Hz
Estimated speed	Optical flow sensor	[0,16]m/s	± 3.5m/S	760 Hz
Speed N/E	GPS	[0, 999] mph	5%	<3s
Global position[3]	GPS	Lat[-90,90]º Lon[-180,180]º	3m	<3s

5.3 Data Analysis

The logged data from different sensors are presented in this section. Data from triad of gyroscopes along body axes of UAV are displayed in Fig. 5, with different colors corresponding to the six flights executed with the same programmed mission in order to visualize the data logged in time. The corresponding boxplots for each flight are shown in Fig. 6, we can appreciate some outliers and no significant biases.

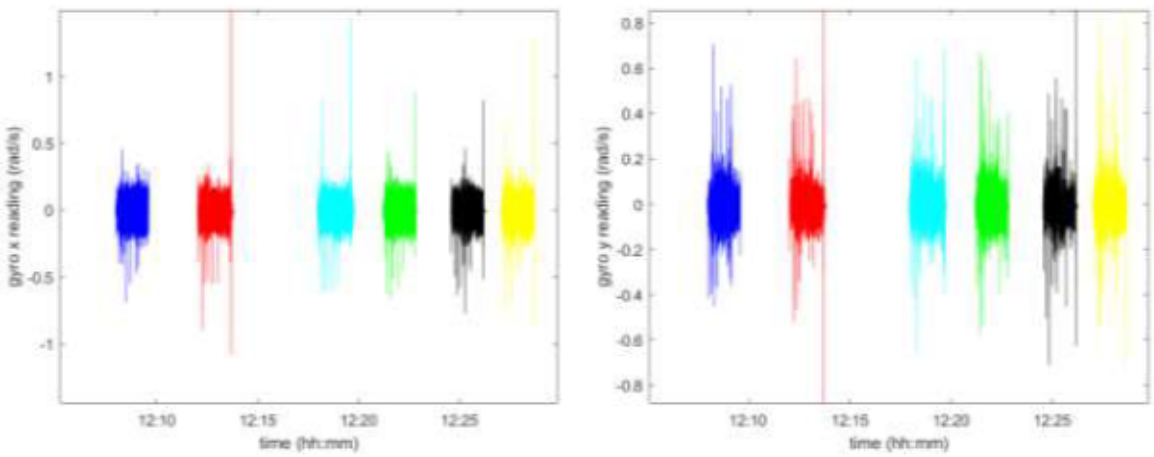

Figure 5: Gyroscope data of test flights (data sequence)

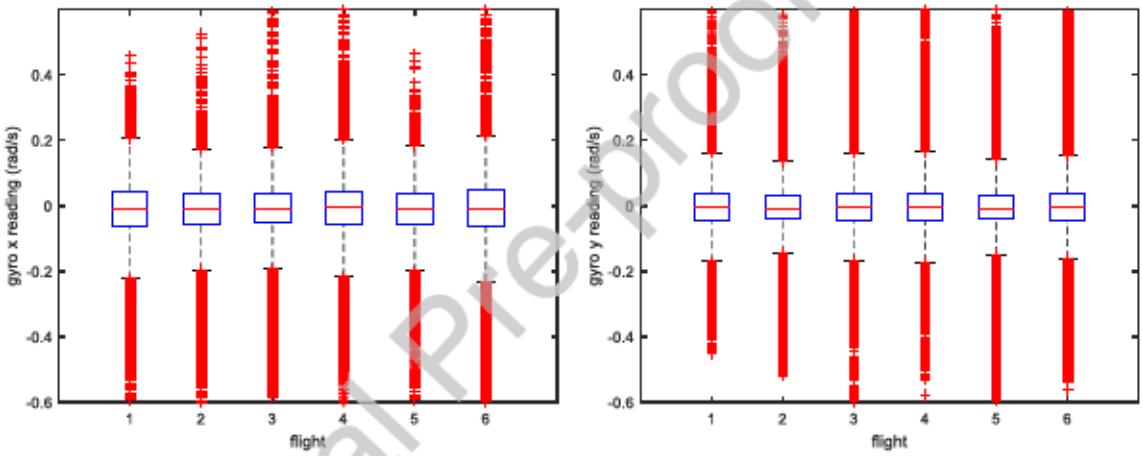

Figure 6: Gyroscope data of test flights (boxplots)

The corresponding histograms of previous data (with outliers removed) are presented in Fig. 7. The analysis of data histograms is important to validate the models of sensor noise, a fundamental element in EKF algorithm. Here we can see the data is affected of Gaussian shape noise, and the mean value of turns corresponding to maneuvers can be seen in the z axis.

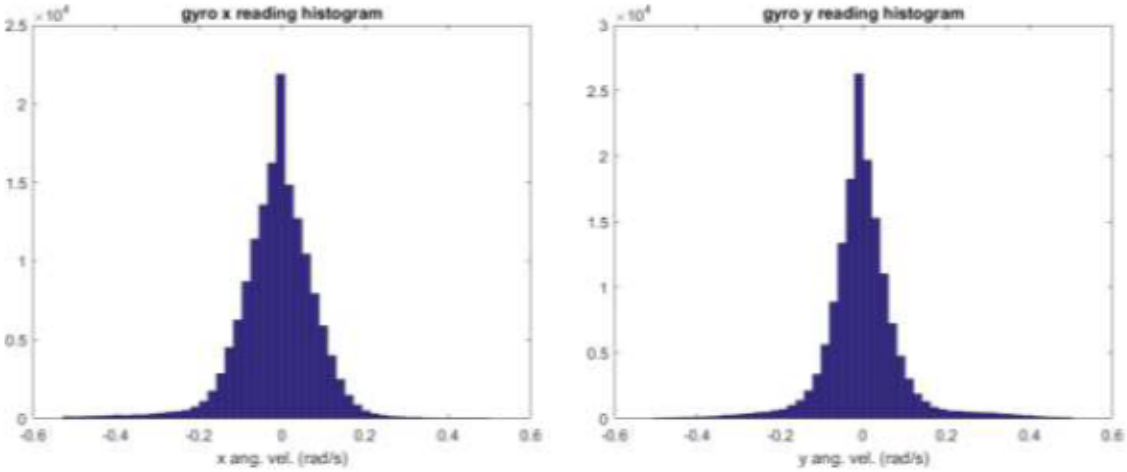

Figure 7: Gyroscope data histograms

Similar comments can be deduced about data from triad of accelerometers, presented in Fig. 8 (boxplots), with some significant outliers which were removed from tracking filter process. The histograms (outliers removed) for the whole set of data in the six flights are presented in Fig. 8.In this case, the turns performed in flights are reflected in the accelerations done along the y axis.

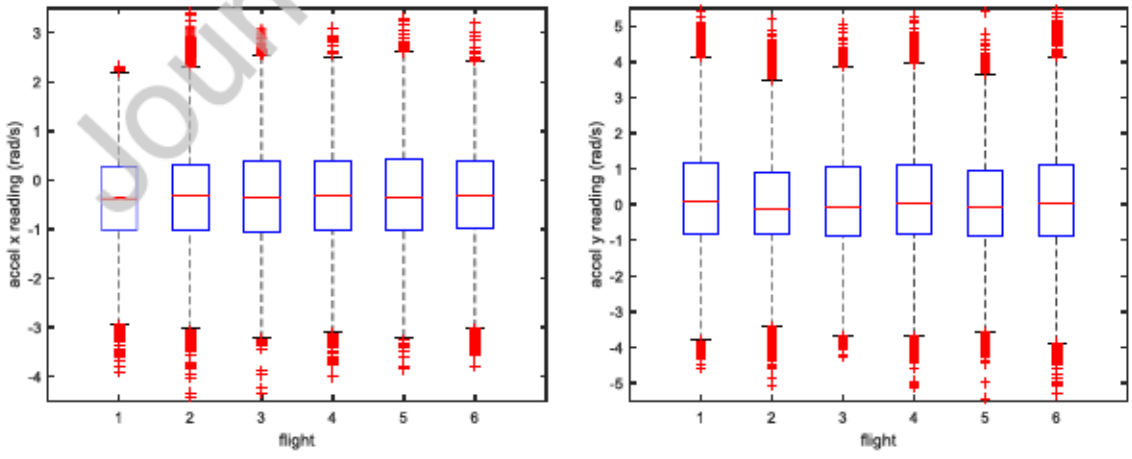

Figure 8: Accelerometer data for all flights (boxplots)

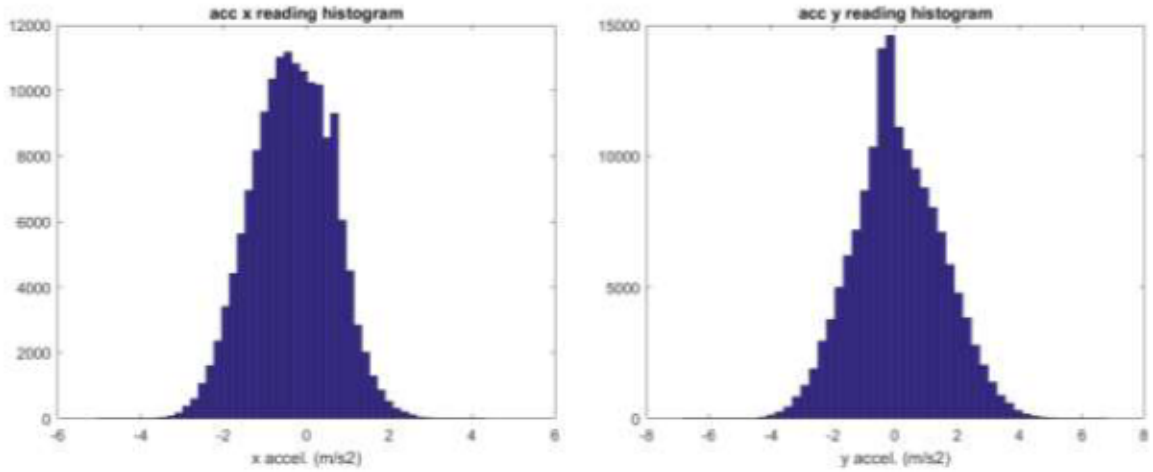

Figure 9: accelerometer data histograms

Similar analysis can be done for the other sensors (magnetometer, barometer, range finder, etc.), not presented here to save space.

5.4 GPS and INS sensor fusion

The most typical task carried out by the data fusion process of the Pixhawk (EKF2 filter) is the attitude estimation using magnetometer, gyroscope and accelerometer data (attitude and heading reference system), and then fuse with accelerometers and GPS data to estimate position and velocity. The EKF2 filter parameters were set using the default values indicated in tables 7,8, except values affecting the performance (table 6), which were analysed accordingly to the methodology presented in this work. The values used for the 6 flights of this mission are indicated in table 11.

The values of prediction errors have been systematically analyzed in the six scenarios considered, with flights repeating the programmed mission (waypoints), but changing the parameters affecting to EKF performance shown in Table 11. The selected values, to analyze the impact on performance metrics appear also in Table 11 and have been set considered the minimum and maximum values recommended in the implemented EKF2 system, being the "default" values (or factory settings) those used in flights #1 and #6.

Table 11. Process Noise Parameters of EKF

Name	Flight1	Flight2	Flight3	Flight4	Flight5	Flight6
EKF2_ACC_B_NOISE	0.003 m/s^3	0.001 m/s^3	0.003 m/s^3	0.007 m/s^3	0.01 m/s^3	0.003 m/s^3
EKF2_GYR_B_NOISE	0.001 rad/s^2	0.001 rad/s^2	0.003 rad/s^2	0.007 rad/s^2	0.01 rad/s^2	0.001 rad/s^2
EKF2_ACC_NOISE	0.35 m/s/s	0.1 m/s/s	0.3 m/s/s	0.7 m/s/s	1.0 m/s/s	0.35 m/s/s
EKF2_GYR_NOISE	0.015 rad/s	0.01 rad/s	0.03 rad/s	0.07 rad/s	0.1 rad/s	0.015 rad/s

The analysis was carried out by postprocessing the data collected from six flight tests using the described UAV system and operated autonomously (besides, the UAV was monitored

remotely by a pilot in visual line of sight for safety reasons). Figure 10 present the horizontal position estimated by tracking filter and GPS observations (circles). As can be appreciated in the zoomed figure 11, the flights corresponding to higher values of parameters (like flight 1, in blue, flight 5, in black) present lower deviations during turns, and, conversely, are affected more by the GPS noise.

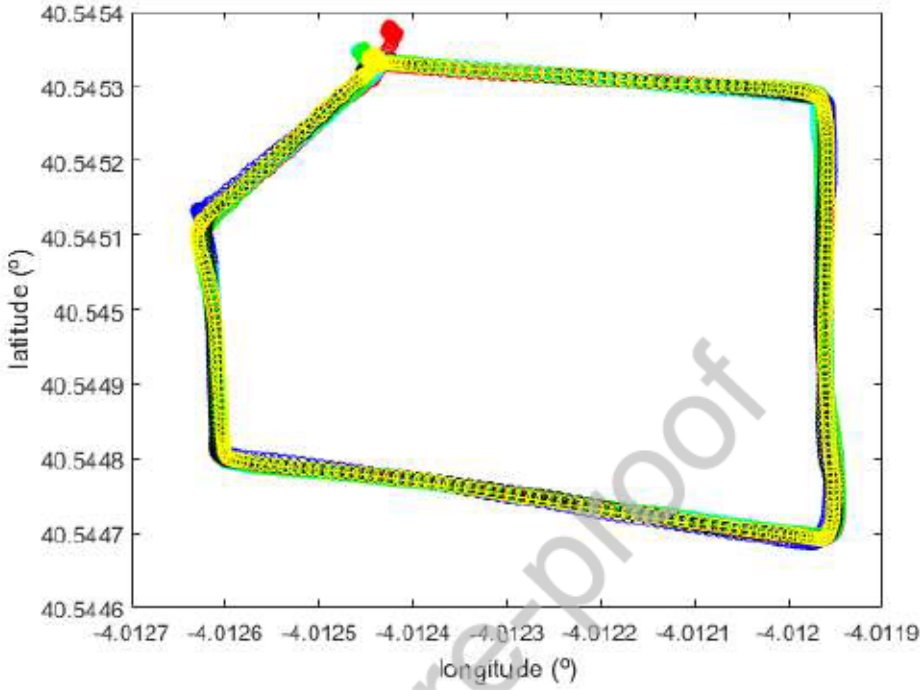

Figure 10: Lat-lon GPS input and EKF output for all flights (1-blue, 2-red, 3-cyan, 4-green, 5-black, 6-yellow)

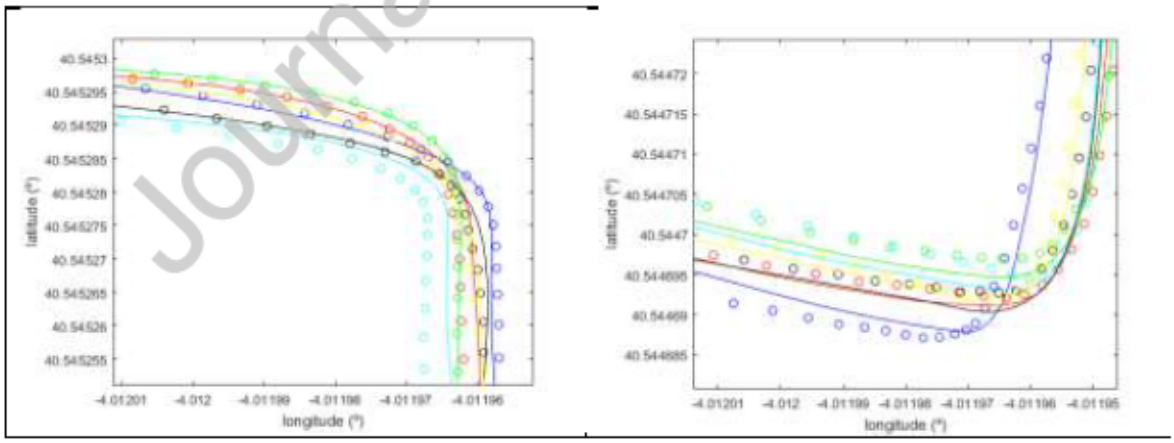

Figure 11: Details of lat-lon GPS input and EKF output for all flights (1-blue, 2-red, 3-cyan, 4-green, 5-black, 6-yellow)

The same effects can be observed with the GPS velocity observations. Figure 12 presents the observations and filtered values, with zoomed graphics for the flights 2 and 6, to appreciate the difference responses of filtered positions with respect to observations.

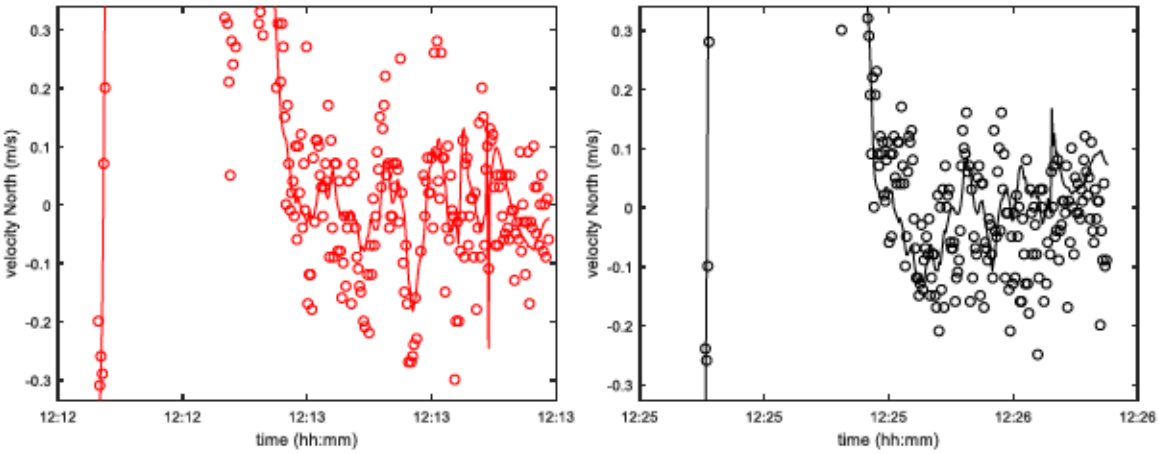

Figure12: Details of lat-lon GPS input and EKF output for two flights (2-red, 5-black)

5.5 Angular orientation

The vehicle orientation is computed based on compass and magnetometer sensors, used to correct the angular estimation based on gyroscopes integrations. Fig. 13 shows the orientation angles (roll, pitch, yaw) with zoomed graphics for flights 2,6. The multi-rotor performs horizontal maneuvers producing rotations around the z axis (yaw), while the pitch and roll reflect the residual noise from control and sensor fusion processes.

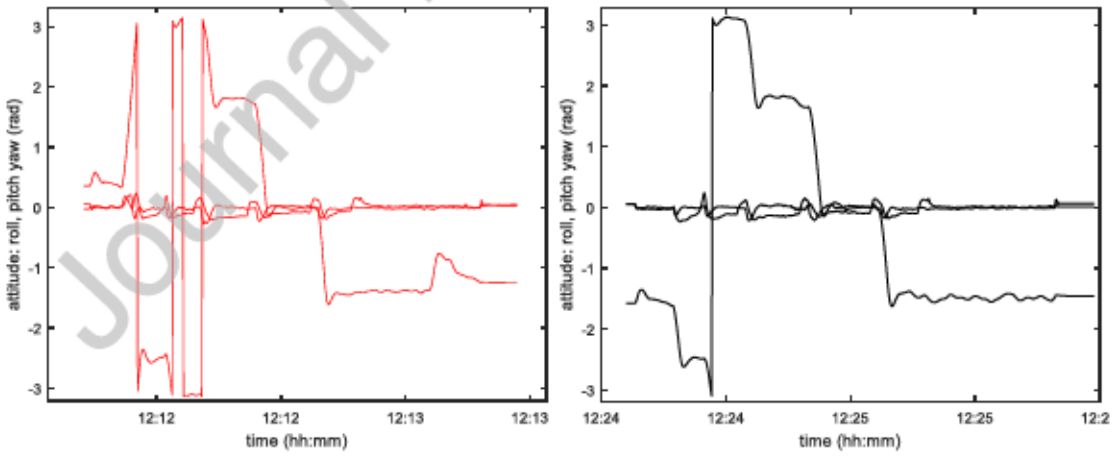

Figure 13: Details of Euler angles for two flights (2-red, 5-black)

5.6 EKF Vertical Filter Performance

Regarding vertical estimation, it can be obtained from different sensors, like barometer, GPS and range finders. Notice that, the GPS value describes a discrete scale with high precision but low resolution and a large latency. On the other side, the barometer measurement allows higher frequency data but requires a calibration with respect to the typical atmospheric pressure. The result of the fusion process throws an estimated value with the accuracy benefits of both measurements, allowing a consistent altitude.

For the flights analyzed in this section, Fig 14 presents the GPS and barometer data input and the estimated outputfor flighs 2 and 5, the weights given to barometer data are higher than GPS, with a smoothing of noise.

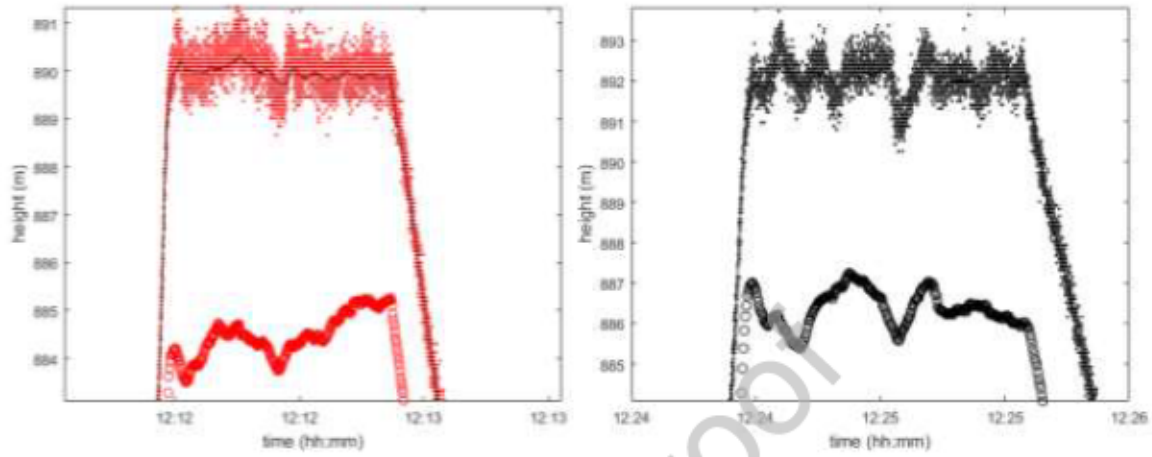

Figure 14: Estimated Details of Barometric and GPS height inputs and EKF output for flights 2-red,5-black

4.7 Analysis of Innovations

The normalized innovations, as presented in section 3, are presented in this section. The position innovations in horizontal plane are presented (their distributions shown as boxplots) in Fig. 15. As can be seen, a slight reduction of values appears in configurations of flights 2 and 4. Similar comments can be appreciated in the velocity innovations, presented in Fig. 16.

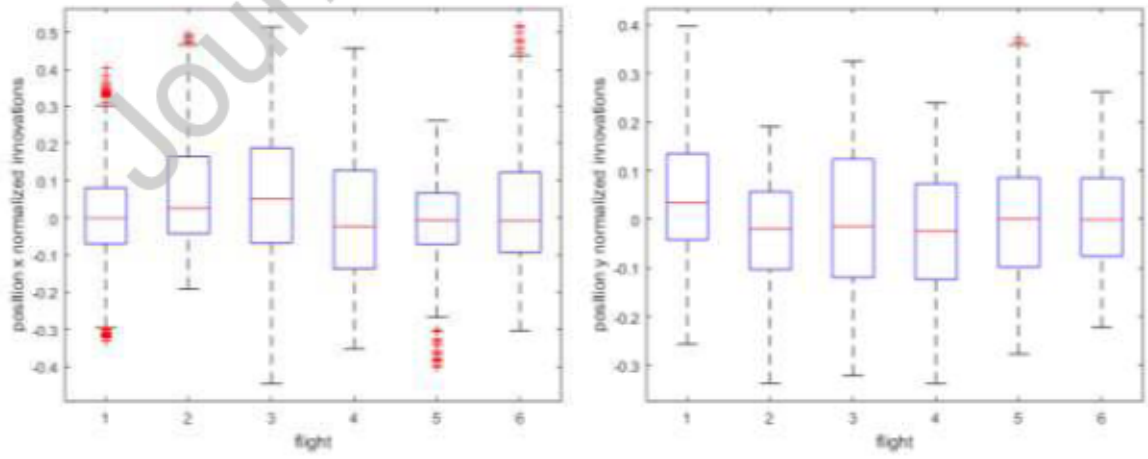

Figure 15: boxplots for position innovations in all flights

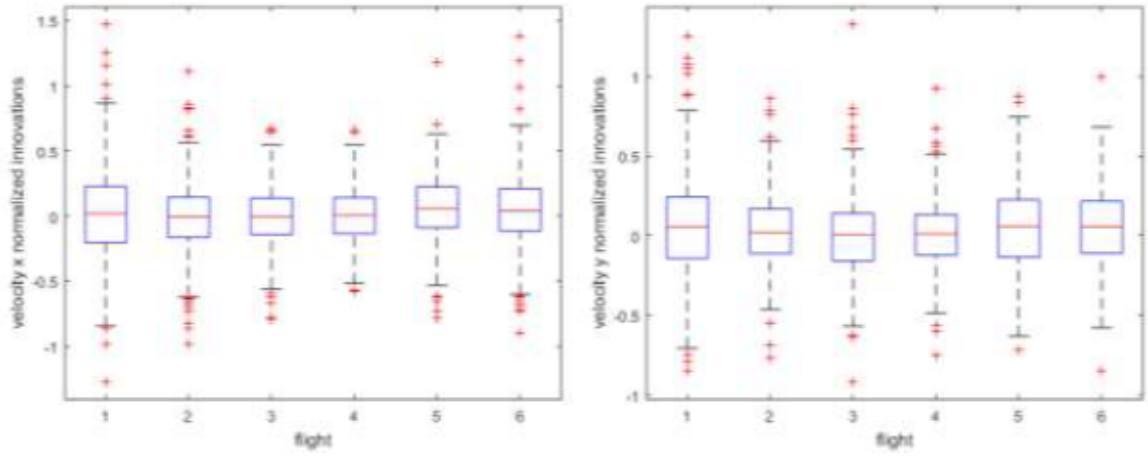

Figure 16: boxplots for velocity innovations in all flights

The accuracy of angular orientation is asessed with magnetometer innovation, the horizontal components are shown in Fig. 17.

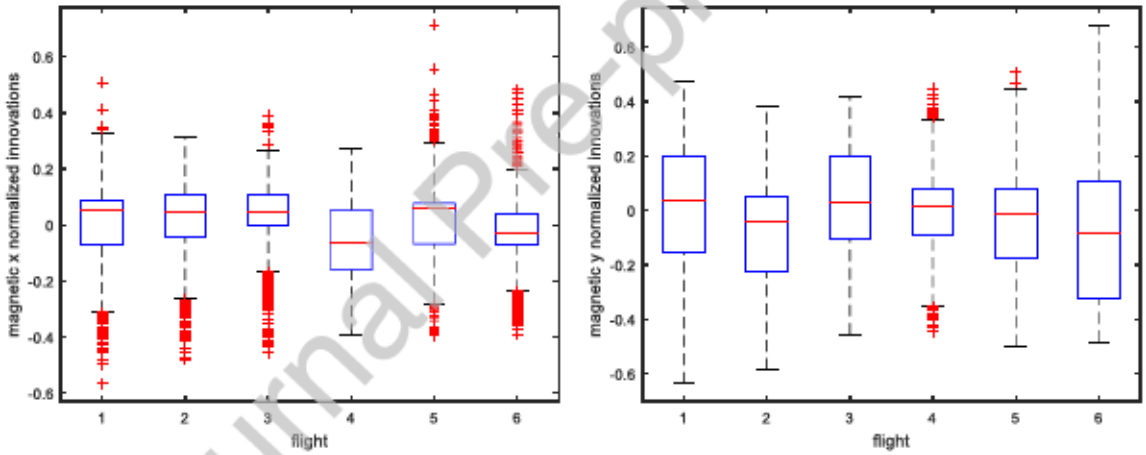

Figure 17: boxplots for orientation innovations

Finally, Figure 18 presents aggregated position, velocity and orientation in a 9D innovation vector, normalized by its covariance matrix. In this case can be seen that flights 3,4 present the lower values.

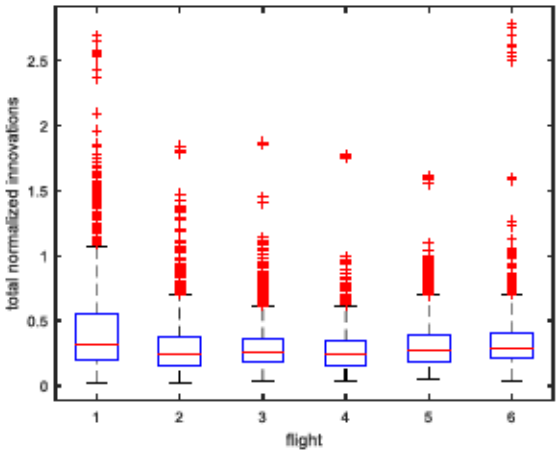

Figure 18: normalized innovations for all flights

This is confirmed with the root mean squared values of innovation, sown in table 12 for the 6 flights

TABLE 12. RMS OF INNOVATIONS

Variable	Flight1	Flight2	Flight3	Flight4	Flight5	Flight6
pos_x	0.1456	0.1786	0.2011	0.1958	0.1205	0.1684
pos_y	0.1366	0.1220	0.1451	0.1368	0.1294	0.1070
pos_z	0.1674	0.1468	0.1452	0.1414	0.1527	0.1651
vel_x	0.3495	0.2583	0.2280	0.2059	0.2517	0.2746
vel_y	0.3250	0.2276	0.2187	0.2025	0.2732	0.2610
vel_z	0.2115	0.1940	0.2226	0.2192	0.2060	0.2172
mag_x	0.1372	0.1167	0.1116	0.1462	0.1309	0.1256
mag_y	0.20357	0.19255	0.19246	0.1733	0.1686	0.2357
mag_z	0.1197	0.1157	0.0952	0.0928	0.1743	0.1058
aggregated pos-vel	0.5210	0.3572	0.3387	0.3084	0.3586	0.4121

4.8 Fusion Breaks

Finally, the fusion logic did not have any fusion break with the different filter parameters tested. The values of tests carried out (innovation divided by five times the standard deviation) are displayed in time in Figure 19, and the distribution represented as boxplots appear are shown in Figure 20.

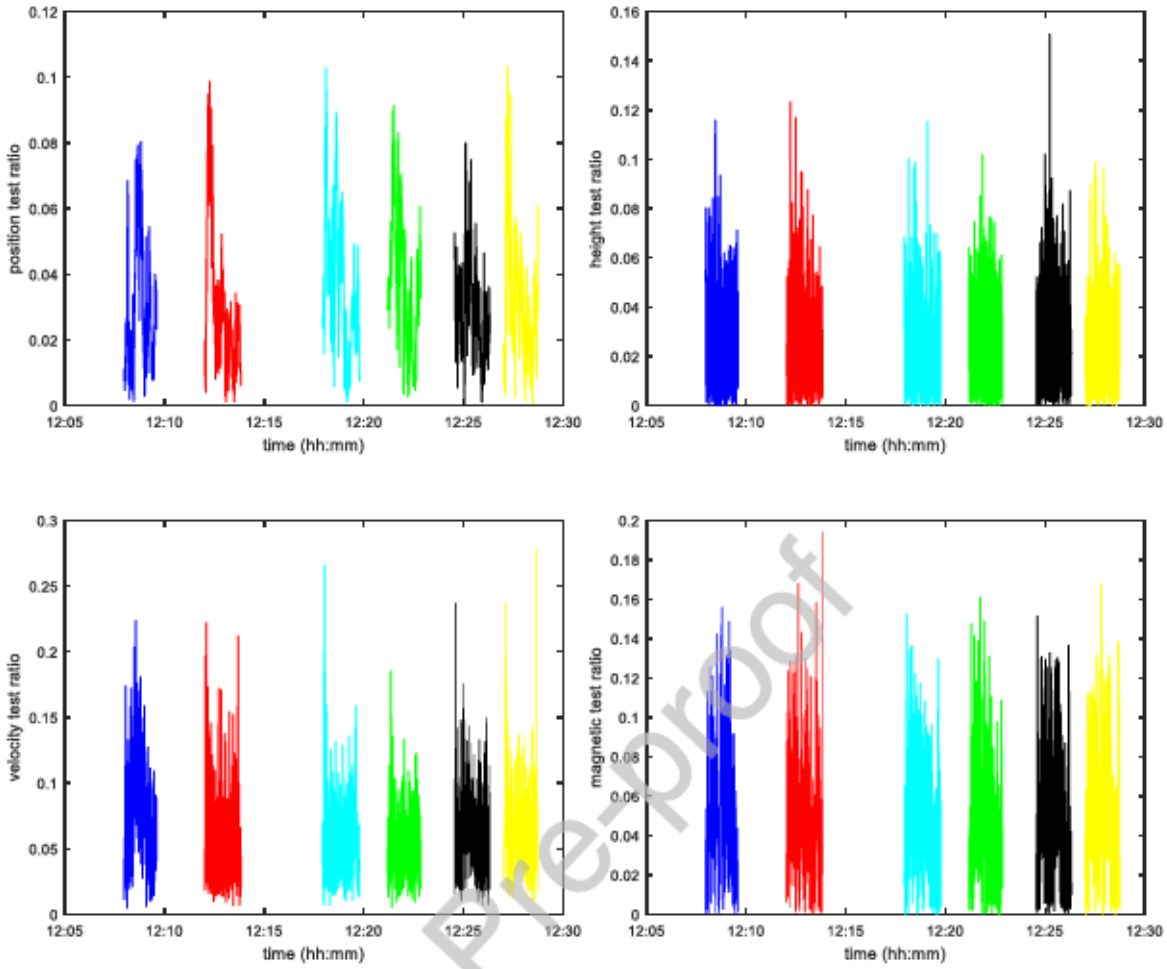

Figure 19: fusion break tests for all flights (horizontal position, height, velocity, attitude)

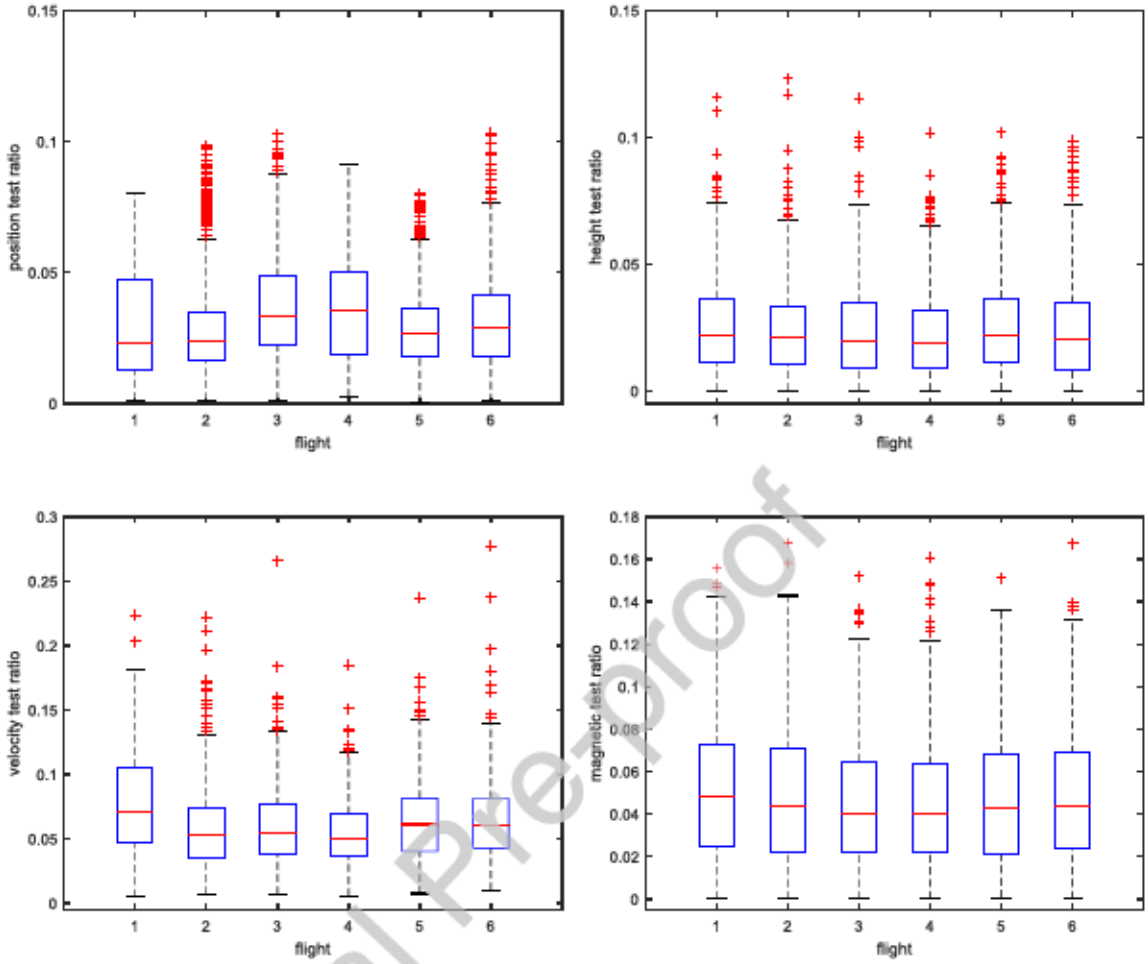

Figure 20: fusion break tests for all flights (horizontal position, height, velocity, attitude)

As commented in section 2.2.1, the distribution of innovations falls within the acceptable conditions of residuals for the assumed error models and none of the observations were discarded in the fusion process to compute the navigation output. The prediction parameters in matrix S show a minimum innovation for the parameters in 4th flight, whose values are not the maximum variance in prediction (the same happens with the aggregated residual). As commented too, an arbitrarily high value of parameters would alow lower values of innovations, but the chi-squared test could be used to dicard those extremely close to zero value.

The results have shown in detail the sensor fusion output with different parameters, reflecting the impact assessed through different magnitues and the quality metrics considered (averaged innovations and fusion breaks). The methodology allows to take decisions of appropriate parameters for the mission considering the global residual of navigation vector and differences with respect to the default configuration (flights #1, #6). A moderate improvement in averaged residuals was appreciated with parameters selected in flight #4, while the robustness in termes of fusion breaks was shown not critically dependent on these parameteres within the recommended intervals. Finally, the methodology can be generalized and applied to different

missions and sets of available sensors to explore the sensitivity of fusion algorithms and find the optimal parameters.

The work presented details an illustrative mission to show the methodology with a use case representing typical missions for monitoring an area (constant height, constant moderate speed between waypints, smooth changes in orientation with coordinated turns). The work will be extended in future to more complex missions to evaluate the best parameters when sharp maneuvers appear in the missions.

A searched result in the mean term will be the best set of configurations for different types of missions, comparing different parameters depending on the characteristics of missions and class of maneuvers (smooth, sharp, etc.). Additionally, an interesting analysis for advanced missions will be the effect on in-flight EKF variation of parameters. For instance, routinary montioring missions can be combined with reactive maneuvers in case of predefined events (identification of unknown objects, obstacle detection and avoidance, etc.). So, although this analysis has been done with a monitoring mission with smooth maneuvers, the final system could have a set of pre-analyzed configurations and switch them accordingly to the current flight mode.

6. Conclusions

This paper presents a platform (Pixhawk PX4) and methodology to experiment with real data and assess the performance of UAV navigation. Based on data analysis and characterization, the algorithms can take advantage of available sources and optimize the performance to provide output with maxium reliability. The quality of all inputs was systematically analyzed, and the parameters of processing algorithms for EKF were evaluated considering the output analysis and specific performance metrics not based on ground truth. The results showed consistency in data with respect to assumed models, sensitivity of accuracy metrics with respect to the key parameters of fusion algorithms, and the possibility of adjusting the system performance to the missions considered. It is an example of the importance of having evaluation evidences to validate the models and assumptions considered in the design.

In summary, this work presents a methodology to test and configure UAV navigation systems in real conditions, illustrated with an open environment for experimentation. The analysis of real data in a systematic way will allow successive improvements and parametrization, considering, among others, the following aspects:

- Data filtering to reduce perturbations and remove outliers
- Quality analysis to weight data uncertainty
- Analysis of biases and calibration before fusion
- Parameter adjustment for other modules (for instance low pass filters or flight control process) to optimize their performance (PID gains, filter parameters, observation and plant noises, etc.)

Acknowledgments

This work was funded by public research projects of Spanish Ministry of Economy and Competitivity (MINECO), references references TEC2017-88048-C2-2-R, RTC-2016-5595-2, RTC-2016-5191-8 and RTC-2016-5059-8

References

[1] Garcia J. Molina J.M., J. Trincado. "Analysis of real data with sensors and estimation outputs in configurable UAV platforms". Sensor Data Fusion: trends, solutions and applications 2017. Bonn, Germany, 10-12 Oct. 2017.

[2] Groves P.D. "Navigation using inertial sensors". IEEE AES Magazine (Vol.30, Iss. 2) 42 - 69 Feb. 2015

[3] Britting, K.R. "Inertial navigation systems analysis". Artech House, 2010

[4] Farrel J.A., "Aided Navigation: GPS with High Rate Sensors", McGraw-Hill, New York, 2008.

[5] Choi H., Kim Y. "UAV guidance using a monocular-vision sensor for aerial target tracking". Control Engineering Practice, 22, 10-19, 2014.

[6] Canedo-Rodríguez A., Álvarez-Santos V., Regueiro C. V., Iglesias R., Presedo J. "Particle filter robot localisation through robust fusion of laser, WiFi, compass, and a network of external cameras". Information Fusion, Volume 27, January 2016, Pages 170-188

[7] Ferrick A., Fish J., Venator E. and Lee G.S. "UAV Obstacle Avoidance Using Image Processing Techniques Technologies for Practical Robot Applications (TePRA", 2012 IEEE International Conference on 23-24 April 2012

[8] Fasano G., Accado D., Moccia A., Moroney D., "Sense and avoid for unmanned aircraft systems". IEEE Aerospace and Electronic Systems Magazine, vol. 31, nº 11, pp. 82-110, 2016.

[9] Rankin G., Tirkel A., Leukhin A. "Millimeter Wave Array for UAV Imaging". MIMO Radar Radar Symposium (IRS), 2015 16th International 24-26 June 2015

[10] Broumandan A., Siddakatte R, Lachapelle G. "An Approach to Detect GNSS Spoofing". IEEE AESS Magazine Vol. 32, N8, August 2017. 64-75

[11] Xiao L., "GNSS Receiver Anti-spoofing Techniques: A Review and Future Prospects". 5th Electronics and Network conference (CECNet 2015) Shanghai, 2015.

[12] Carson N., Martin S.M., Starling J., and Bevly D.M. "GPS Spoofing Detection and Mitigation Using Cooperative Adaptive Cruise Control System". 2016 IEEE Intelligent Vehicles Symposium (IV) Gothenburg, Sweden, June 19-22, 2016. 1091-1096

[13] Blasch E., Pribilski M., Daughtery B., Roscoe B., and Gunsett J., "Fusion Metrics for Dynamic Situation Analysis," Proc. SPIE 5429, April 2004.

[14] Kim J., Cheng J., Guivant J., Nieto J., "A. Compressed Fusion of GNSS and Inertial Navigation with Simultaneous Localization and Mapping". IEEE AESS Magazine Vol. 32, N8, August 2017. 22-36

[15] Sun R., Cheng Q., Wang G. and Ochieng W.Y. "A Novel Online Data-Driven Algorithm for Detecting UAV Navigation Sensor Faults". Sensors 2017, 17(10), 2243;

[16] Gao W., Zhang Y. and Wang J." A Strapdown Interial Navigation System/Beidou/Doppler Velocity Log Integrated Navigation Algorithm Based on a Cubature Kalman Filter". Sensors 2014, 14(1), 1511-1527

[17] David Gualda, Jesús Ureña, Juan C. García, Enrique García, José Alcalá. Simultaneous calibration and navigation (SCAN) of multiple ultrasonic local positioning systems. Information Fusion, Volume 45, January 2019, Pages 53-65

[18] Yao Y. and Xu X. "A RLS-SVM Aided Fusion Methodology for INS during GPS Outages". Sensors 2017, 17(3).

[19] Jing Li, Ningfang Song, Gongliu Yang, Ming Li, Qingzhong Cai. Improving positioning accuracy of vehicular navigation system during GPS outages utilizing ensemble learning algorithm. Information Fusion, Volume 35, May 2017, Pages 1-10

[20] Rhudy M.B., Gross J.N., Chao H., "Onboard Wind Velocity Estimation Comparison for Unmanned Aircraft Systems". IEEE Transactions on Aerospace and Electronic Systems, Vol. 53, N.1, Feb 2017, pp 55-66.

[21] Jiang C., Zhang S.B. and Zhang Q.Z. "A New Adaptive H-Infinity Filtering Algorithm for the GPS/INS Integrated Navigation". Sensors 2016, 16(12), 2127

[22] Martí E., García J., Molina J.M. "A Simulation Framework for UAV Sensor Fusion". Hybrid Artificial Intelligence Systems 5th International Conference, HAIS 2010, San Sebastián, Spain, June 23-25, 2010.

[23] Layh T., Demoz G.E. "Design for Graceful Degradation and Recovery from GNSS Interruptions", IEEE AESS Magazine Vol. 32, N9, September 2017. 4-17.

[24] Ng, G., Tan, C., Ng, T., & Siow, S. "Assessment Of Data Fusion Systems". In 2006 9th International Conference on Information Fusion (pp. 1–8). 2006.

[25] Tan, C. H., Chen, H., & Ng, G. W. "Assessment of data fusion systems part 2: Sensor network architectures". 13th International Conference on Information Fusion, 2010.

[26] Gorji, A.A., Tharmarasa, R., and Kirubarajan, T. "Performance measures for multiple target tracking problems". 14th International Conference on Information Fusion. Chigaco, USA, July 2011.

[27] Schubert, R., & Klöden, H. " Performance evaluation of Multiple Target Tracking in the absence of reference data". 13th International Conference on Information Fusion, 2010.

[28] Zhang, L., Lan, J., & Li, X. R. A Fused Score for Ranking and Evaluation Using Multiple Performance Metrics", 19th International Conference on Information Fusion, 2016.

[29] Blasch, E. P., Pribilski, M., Daughtery, B., Roscoe, B., & Gunsett, J. "Fusion metrics for dynamic situation analysis". Proceedings of SPIE - The International Society for Optical Engineering, 5429(April), 428–438. (2004).

[30] Rawat, S., Llinas, J., & Bowman, C. "Design of a Performance Evaluation Methodology for Data Fusion-based Multiple Target Tracking Systems". Presented at the SPIE Aerosense Conference, Orlando, FL, April, 5099, 139–151. (2003).

[31] Hermans, F., Dziengel, N., & Schiller, J. "Quality estimation based data fusion in wireless sensor networks". 2009 IEEE 6th International Conference on Mobile Adhoc and Sensor Systems (pp. 1068–1070). (2009).

[32] Bisdikian, C. " On Sensor Sampling and Quality of Information: A Starting Point". In Fifth Annual IEEE International Conference on Pervasive Computing and Communications Workshops, 2007. PerCom Workshops '07 (pp. 279–284).

[33] Colegrove, S. B., Bldg, I. B., Cheung, B., & Davey, S. J. (2003). "Tracking System Performance Assessment". 6th International Conference on Information Fusion, 926–933, Queensland, Australia, July 2003

[34] García J., Molina J.M., Besada J.A., de Miguel G. "Model-Based Trajectory Reconstruction with IMM Smoothing and Segmentation". Information Fusion Vol. 22 (2015) 127-140

[35] García, J., Luis, Á., Molina, J. M. "Quality-of-service metrics for evaluating sensor fusion systems without ground truth". 19th International Conference on Information Fusion, Heidelberg, Germany, July 2016.

[36] Besada J.A., Garcia J., Miguel G., Soto A., Voet E. "ATC trajectory reconstruction for automated evaluation of sensors and trackers performance". IEEE Aerospace and Electronic Systems Magazine Vol. 28 (2013) 4-17.

[37] Guerrero J.L., García, J., Molina, J.M. "Piecewise Linear Representation Segmentation in Noisy Domains with a Large Number of Measurements: The Air Traffic Control Domain". International Journal on Artificial Intelligence Tools (2011) 20(2), 367-399.

[38] Khaleghi B., Khamis A., Karray F.O., Razavi S.N., "Multisensor data fusion: A review of the state-of-the-art". Information Fusion Volume 14, Issue 1, January 2013, Pages 28–44

[39] Babister, A. W. (1980). "Aircraft dynamic stability and response" (1st ed.). Oxford: Pergamon Press. ISBN 978-0080247687.

[40] Martí E., García J., Escalera A., Molina J.M., Armingol J.M. "Context-Aided Sensor Fusion for Enhanced Urban Navigation". Sensors Vol. 2012 16802-16837.

[41] Ndjeng Ndjeng, A.; Gruyer, D.; Glaser, S.; Lambert, A. Low Cost IMU–Odometer–GPS Ego Localization for Unusual Maneuvers. Information Fusion 2011, 12, 264-274.

[42] Caron, F.; Duflos, E.; Pomorski, D.; Vanheeghe, P. "GPS/IMU Data Fusion using Multisensor Kalman Filtering: Introduction of Contextual Aspects". Information Fusion 2006, 7, 221-230.

[43] Noureldin, A.; El-Shafie, A.; Bayoumi, M. GPS/INS "Integration utilizing Dynamic Neural Networks for Vehicular Navigation". Information Fusion 2011, 12, 48-57.

[44] R. vd Merwe; E.A. Wan, S.I. Julier. Sigma-Point Kalman Filters for Nonlinear Estimation and Sensor-Fusion Applications to Integrated Navigation. AIAA Guidance, Navigation and Controls Conference, Providence, RI USA, August 2004.

[45] Hyyti H. and Visala A., "A DCM Based Attitude Estimation Algorithm for Low-Cost MEMS IMUs". International Journal of Navigation and Observation, Volume 2015, Article ID 503814.

[46] Meier L., PX4 Development Guide. [Online]. Available: https://dev.px4.io/en/

CRediT author statement

Jesus Garcia: Conceptualization, Validation, Writing, Investigation, Software

José Manuel Molina.: Supervision, Writing Revieweing, Methodology.

Jorge Trincado: Data curation, Software, Investigation, Original Draft Preparation

Declaration of Competing Interest

The authors whose names are listed immediately below certify that they have NO affiliations with or involvement in any organization or entity with any financial interest (such as honoraria; educational grants; participation in speakers' bureaus; membership, employment, consultancies, stock ownership, or other equity interest; and expert testimony or patent-licensing arrangements), or non-financial interest (such as personal or professional relationships, affi liations, knowledge or beliefs) in the subject matter or materials discussed in this manuscript

The authors whose names are listed immediately below report the following details of affi liation or involvement in an organization or entity with a financial or non-financial interest in the subject matter or materials discussed in this manuscript. Please specify the nature of the conflict on a separate sheet of paper if the space below is inadequate.